

Research Article

MATHEMATICAL APPRECIATION ON MANAGEMENT OF CONDYLAR FRACTURE AT ELBOW-JOINT

***Swapan Kumar Adhikari**

*Ex-Head of an Educational Institution; 35/1, Krishnataran Naskar Lane, Howrah - 711107,
West Bengal, India*

**Author for Correspondence*

ABSTRACT

The distal condyles of humerus have characteristic orientation with reference to diaphysis. In adults anatomical reduction does not restore pre-injury functional status of the articular surface. The purpose of this study is to determine mathematically the outcome of treating the condylar fractures with pre-contoured plates and suggest proper functional alignment of distal humerus; mathematical modelling of better alignment.

Key Words: *Condylar Fracture, Carrying Angle, Geodesic, Moment, Spiral*

INTRODUCTION

We have examined distal condyle of humerus mathematically; in particular from geometrical view point. Mechanical behaviour of structure along with mechanical ability of plates and screws has been considered.

DISCUSSION

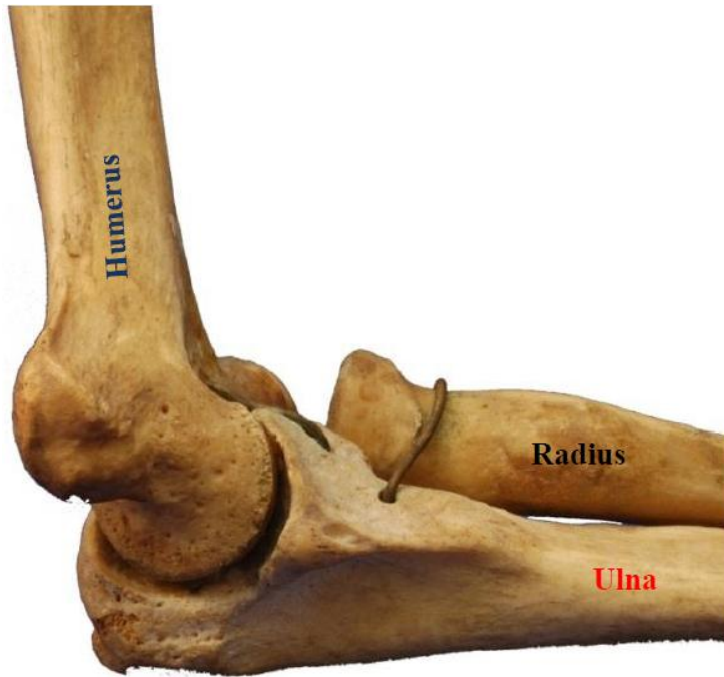


Figure 1: Humerus, ulna, radius joint

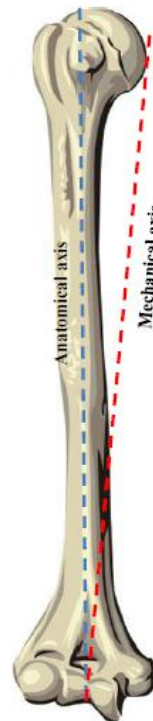


Figure.2: Right Humerus

Egyptians were earliest people who started hand surgery more than 4,500 years ago as documented in The Edwin Smith Papyrus. Orthopaedics has since developed in the hands of clinicians and orthopaedic surgeon (Breasted, 1930).

Research Article

(a) Mathematical Examination of Elbow Joint Structure

Figure 2 shows the mechanical axis for transmission of force through humerus and also the anatomical axis for geometrical representation.

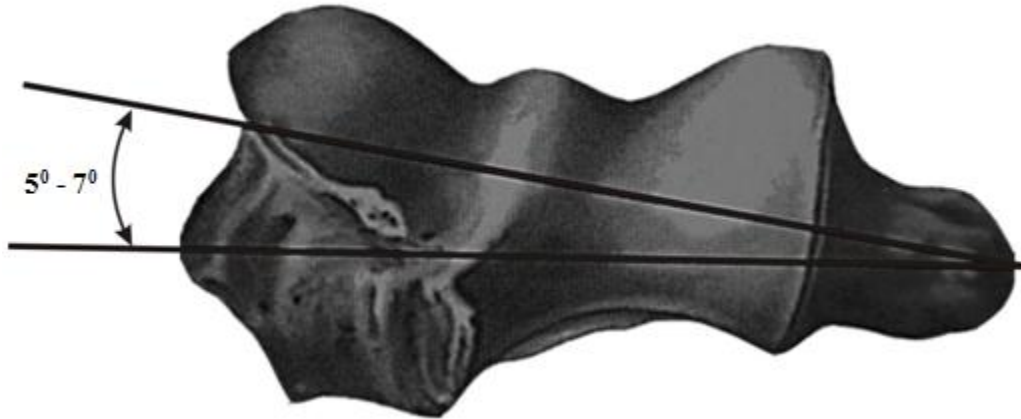


Figure 3: Trochlea has 5° - 7° internal rotation with reference to the line mid portions of epicondyles

Trochlear groove is spiral (Figure 3) it has medial and lateral portions. The medial projects more than lateral portion. Thus an angle of about 6° in men and 10° in women is created between central axis and line connecting centre of projected portion to the centre of capitulum which is called valgus-angle (δ , delta) (Figure 9) (Adhikari *et al.*, 2011).

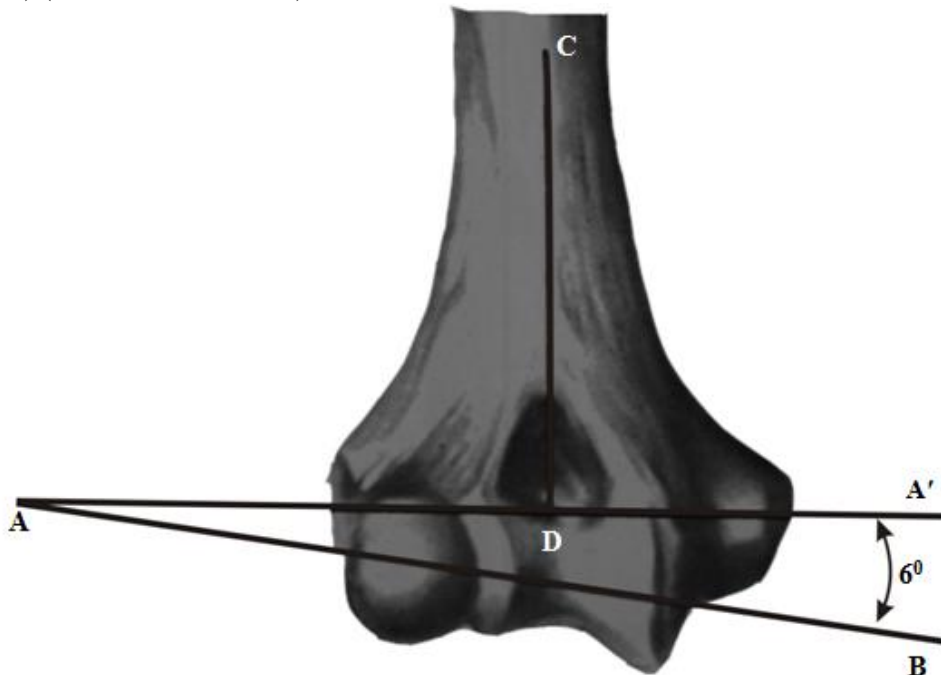


Figure 4: Nearly on an average of 6° valgus in respect of epicondylar axis perpendicular to long axis of the left humerus

Trochlea is also provided with a hemispherical capitulum which is placed laterally. This facilitates supination and pronation. The complex formed by capitulum and trochlea is like a ball and spool as if threaded in the same axis AB (Figure 4) which is the axis of flexion and extension of elbow.

Research Article

Trochlear surface is not perfectly cylindrical but a sellar (multi-centre spheroidal) thus it can manage with lesser friction between the bones at the time of movement of ulna over trochlea. Coronoid and radial fossae of distal end of humerus accommodate olecranon of ulna.

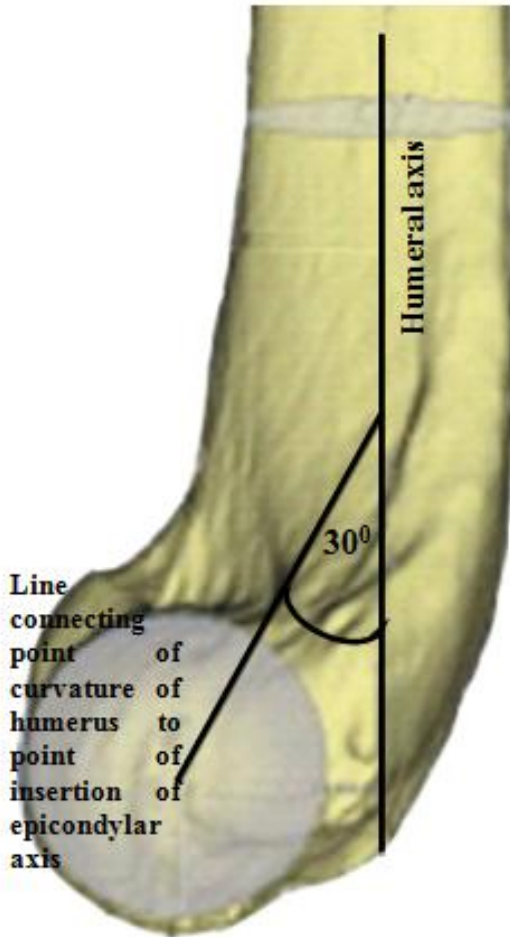


Figure 5: Angle of inclination epicondylar axis to the humeral axis

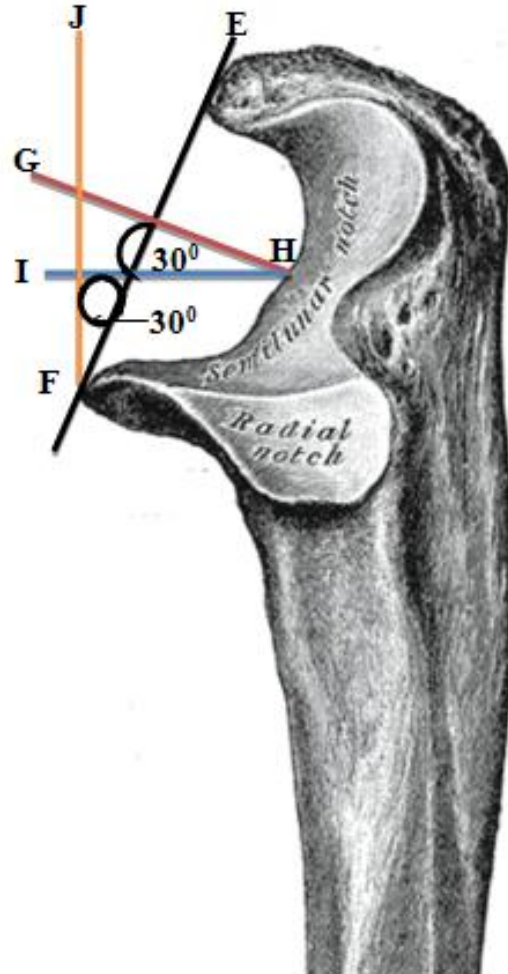


Figure 6: Proximal part of ulna demonstrating angular difference between coronoid process and olecranon. EF = line joining olecranon and coronoid process; GH = line perpendicular to EF; IH = horizontal line determining angulation; FJ = vertical line at F

Semilunar notch of the ulna with average 30° backward angles (Figure 6) fit with 30° extended angle of trochlea-capitulum (Figure 5). This articulation also keeps enough gaps for full extension of ulna-radius with humerus which nearly 172° (Figure 8). In other words we may say distal end of humerus anteriorly bulges an average angle of 30° with the shaft (Figure 5) to accommodate it, trochlear notch of ulna holds an average angle of 30° anterior-posteriorly and these arrangement gives a mechanical advantage on free as well as smooth rotation of ulna about epicondylar axis of trochlea-capitulum.

The carrying angle of the elbow (Figure 7A): The forearm lies slightly laterally to the humerus when elbow is fully extended in the anatomical position. Figure 7B: The long axis of the humerus and the long axis of the forearm subtend the carrying angle Ω (omega) and it depends on the valgus angle δ (delta) of the trochlea (Figure 9).

Research Article

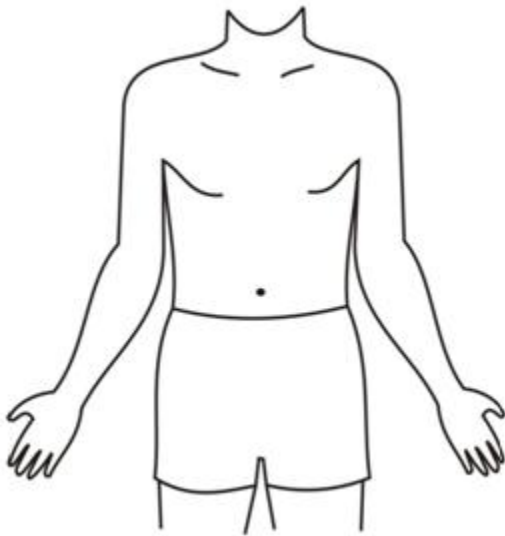


Figure 7A: Showing carrying angle

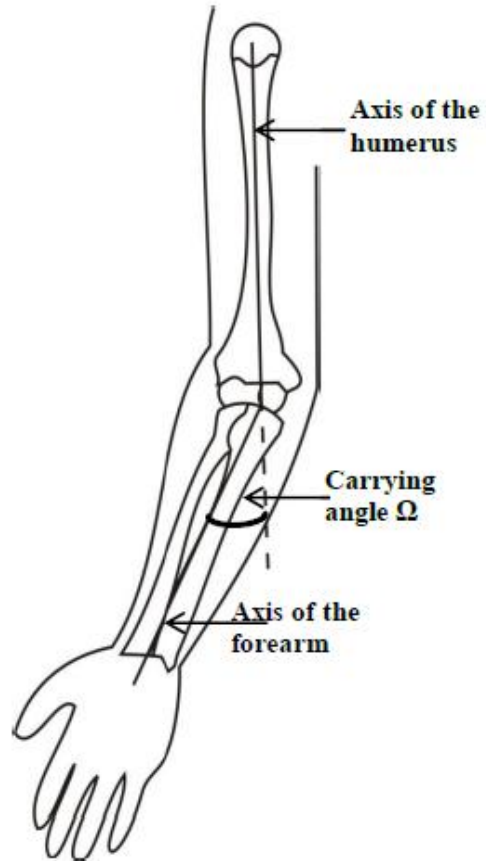


Figure 7B: Indicating carrying angle

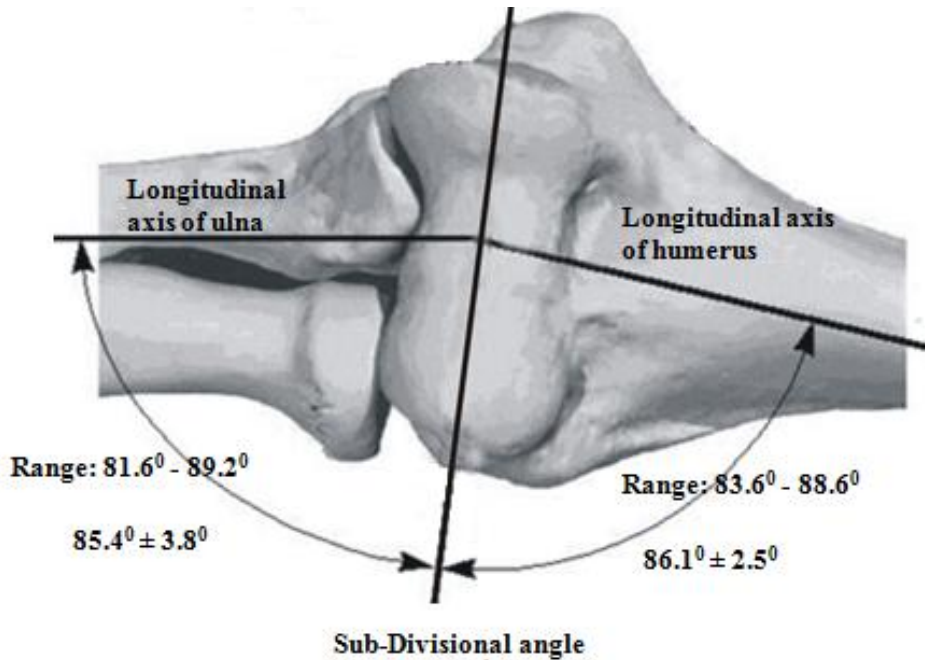


Figure 8: Angulation of humerus and ulna with respect to axis of trochlea

Research Article

In extension, (Figure 8) (i) average angle between longitudinal axis of ulna & trochlear axis = $(81.6^\circ + 89.2^\circ) \div 2 = 85.4^\circ$ and (ii) average angle between longitudinal axis of humerus & trochlear axis = $(83.6^\circ + 88.6^\circ) \div 2 = 86.1^\circ$. Therefore, average extension angle = $85.4^\circ + 86.1^\circ = 171.5^\circ \approx 172^\circ$ as assumed under figure 13A.

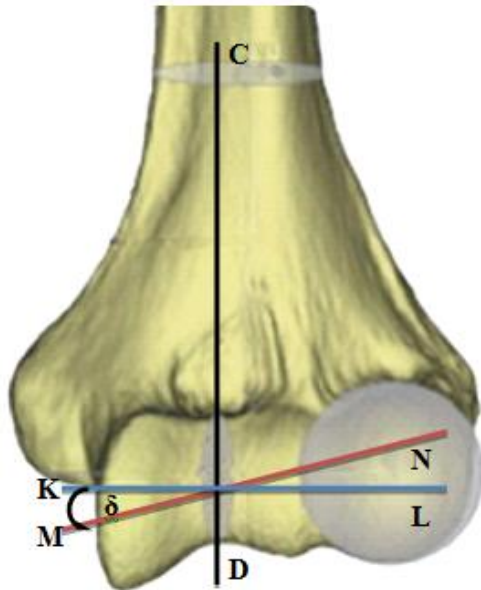


Figure 9: Showing medial and lateral Figure 10: Anterior view of ulna showing supracondylar columns, trochlea and capitulum of humerus trochlear ridge

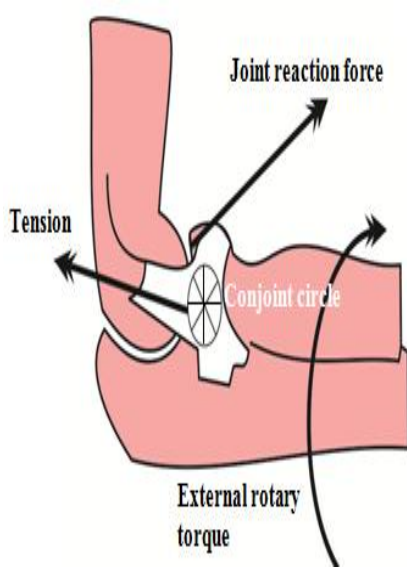


Figure 11A: Lateral view

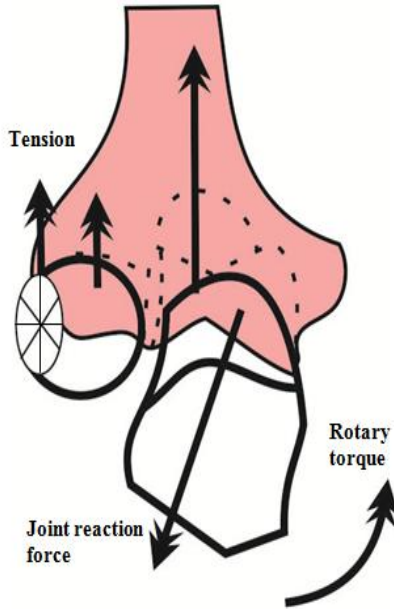


Figure 11B: Anterior view

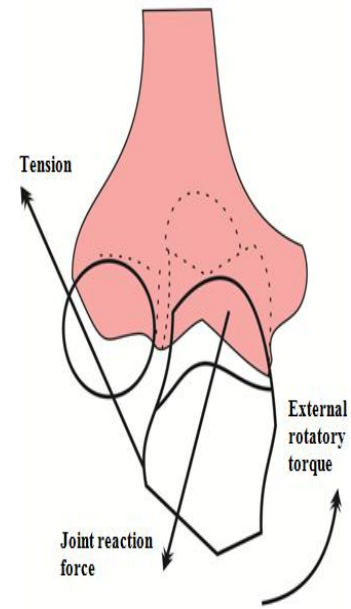


Figure 11C: Anterior without showing anterior band

(b) Forces Acting for Joint-Stability

Joint-stabilising mechanism with a conjoint point under external rotary torque can be demonstrated by Figures.11A & 11B. Tension of the 3 bands connecting humerus, radius and ulna with central conjoint

Research Article

point (circle) stabilizes the radioulnar, radiohumeral, and ulnohumeral joints simultaneously. The conjoint point is fixed on the radial head and behaves as an insertion to the ulna here. Lateral view (Figure 11A) and anterior view (Figure 11B) of the elbow joint-stabilising mechanism include the joint reaction forces and ligamentous tension.

Restraint against posterolateral rotatory torque due to severance of the anterior band is shown in Figure 11C. Here joint congruity does not remain intact. Without the effect of tension by the anterior band, laxity at the proximal radioulnar joint may be observed.

A joint reaction force from the trochlea to the coronoid process prevented frank dislocation of the ulnohumeral joint with tension of fibers connecting the epicondyle of the humerus to the proximal ulna.

(c) Mechanics of Normal Movement

We find that movements on the spirally curved surface is effective in two axes (a) axis perpendicular to the humeral axis CD i.e. KL; (b) axis perpendicular to the tangent of the spiral i.e. MN (Figure 9). Here KL and MN subtends δ = varus-valgus angle of trochlea.

In flexion axis of movements is as per (a) and in extension it is as per (b) by which it extend to carrying angle. This carrying angle is Ω which is the valgus angle of the trochlea. In men it is $5^\circ - 7^\circ$ whereas in women it is $8^\circ - 12^\circ$. Here δ is known as varus-valgus angle.

This trochlear ridge (Figure 10) is slightly curved anteriorly to move over spiral-groove over trochlea for sliding in flexion and extension.

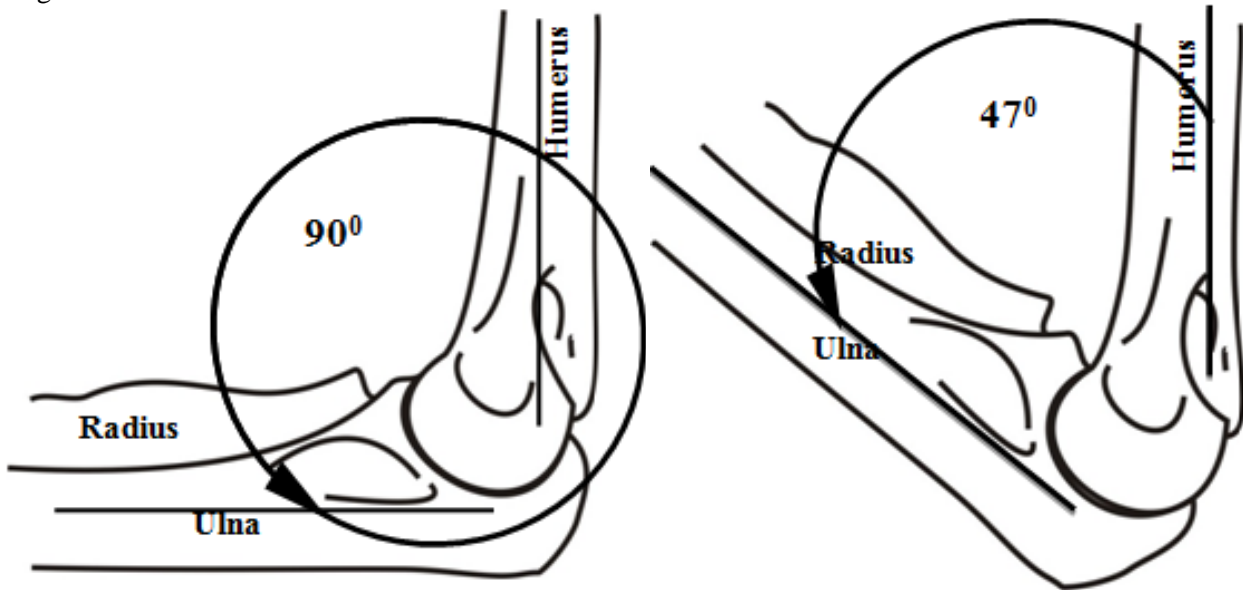


Figure 12A: 90° flexion showing ulnar movement

Figure 12B: Full flexion showing ulnar movement

In flexion, the trochlear ridge of ulna slides along the spiralic trochlear groove until the coronoid process reaches the floor of the coronoid fossa for full flexion.

There exists physiologic incongruity between the articulating surfaces of trochlea and its notch for load reduction. Rim of the radial head slides in the capitulotrochlear groove and enters the radial fossa to complete flexion. In extension, there is no contact occurs between articulating surfaces.

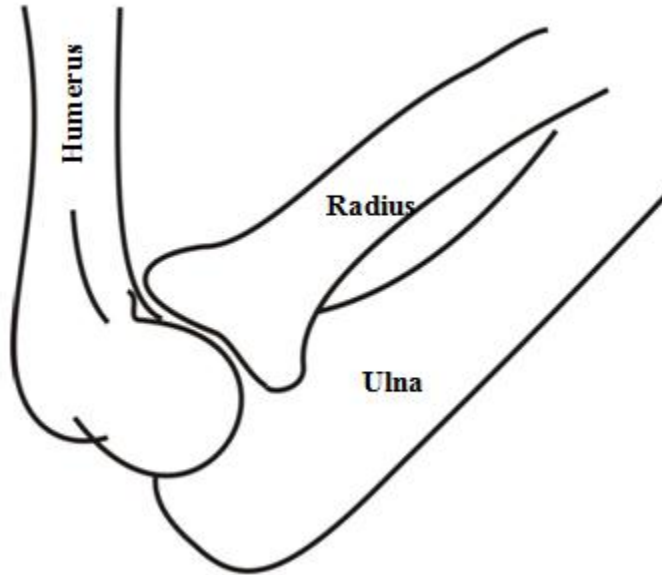


Figure 12C: Full flexion showing radial movement

Above schematic figures are expressing positions of humerus-ulna-radius joint movements in flexion is nearly 125° ($172^\circ - 47^\circ$) (Figure 12B) after extension where extension angle is 172° (Figure 13A & 13B).

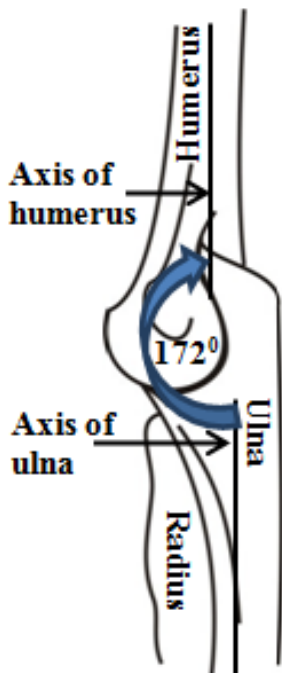


Figure 13A: Extension showing ulna

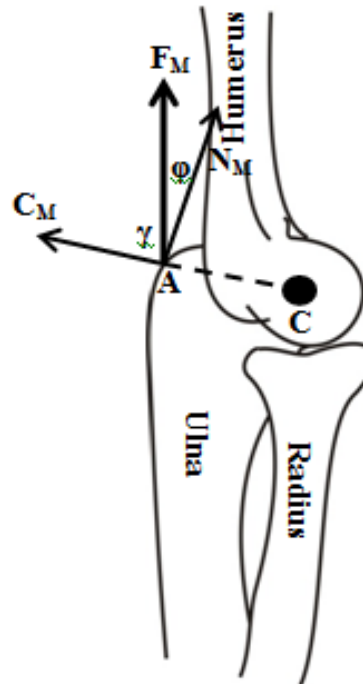


Figure 13B: Extension showing radius

In full extensor muscular force (F_M) exerted, at A, can resolved into (a) centrifugal force (C_M) from centre C through A and (b) normal component (N_M) towards humerus. Here for extension $N_M \gg C_M$ as $\phi \ll \gamma$ as well as $\cos \phi > \cos \gamma$ and $N_M = F_M \cdot \cos \phi$; $C_M = F_M \cdot \cos \gamma$ where $\phi + \gamma = 90^\circ$ (Figure 13B).

So, extensor muscle helps to (a) keep radio-ulnar complex attached with humerus rigidly by N_M ; (b) extend radio-ulnar complex by C_M .

Research Article

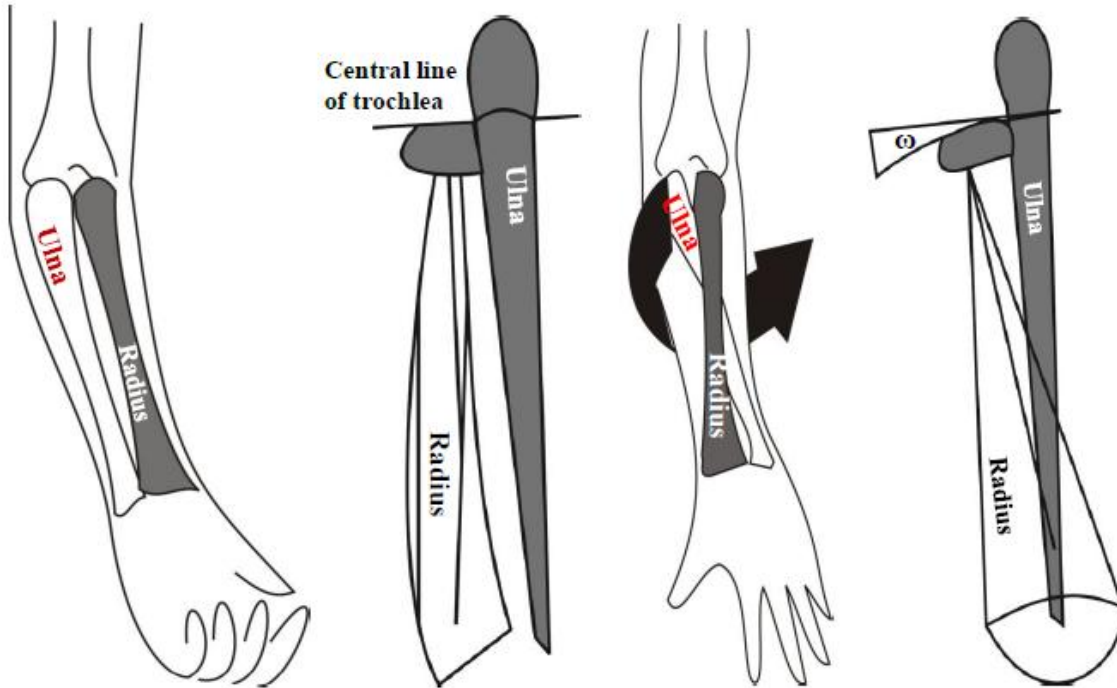


Figure 14A: Supination of forearm **Figure 14B: Schematic diagram of supination** **Figure 14C: Pronation of forearm** **Figure 14D: Schematic diagram of pronation**

(d) Supination and Pronation

In supination (Figure 14A): In forearm radius and ulna are parallel to each other whereas in pronation (Figure 14C): the radius crosses the ulna. These activity is only possible due to spheroidal structure of capitulum along with valgus position of trochlea such that radius can turn smoothly over capitulum. In schematic diagrams we see for supination (Figure 14B) radius lie by the side of ulna i.e. axis of the radius is parallel to ulna and move with it as these are attached to each other i.e. along with the movement of ulnar ridge over the spiral on the surface of trochlea, the radius also move same way on the capitulum. But in pronation (Figure 14D) the radius move on the spherical surface of capitulum when its distal end move to form a cone and naturally it overlaps ulna.

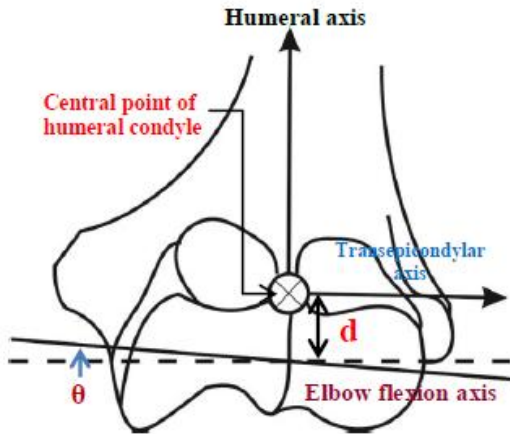


Figure 15A: Medial view of the distal humerus

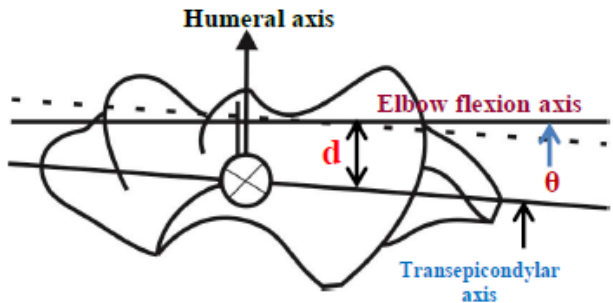


Figure 15B: Superior view of the distal humerus

Research Article

So long axis of radius runs obliquely distally and medially. Then plane of the radial head, which is perpendicular to radial axis, is tilted distally and laterally at an angle ω (omega) with the horizontal plane.

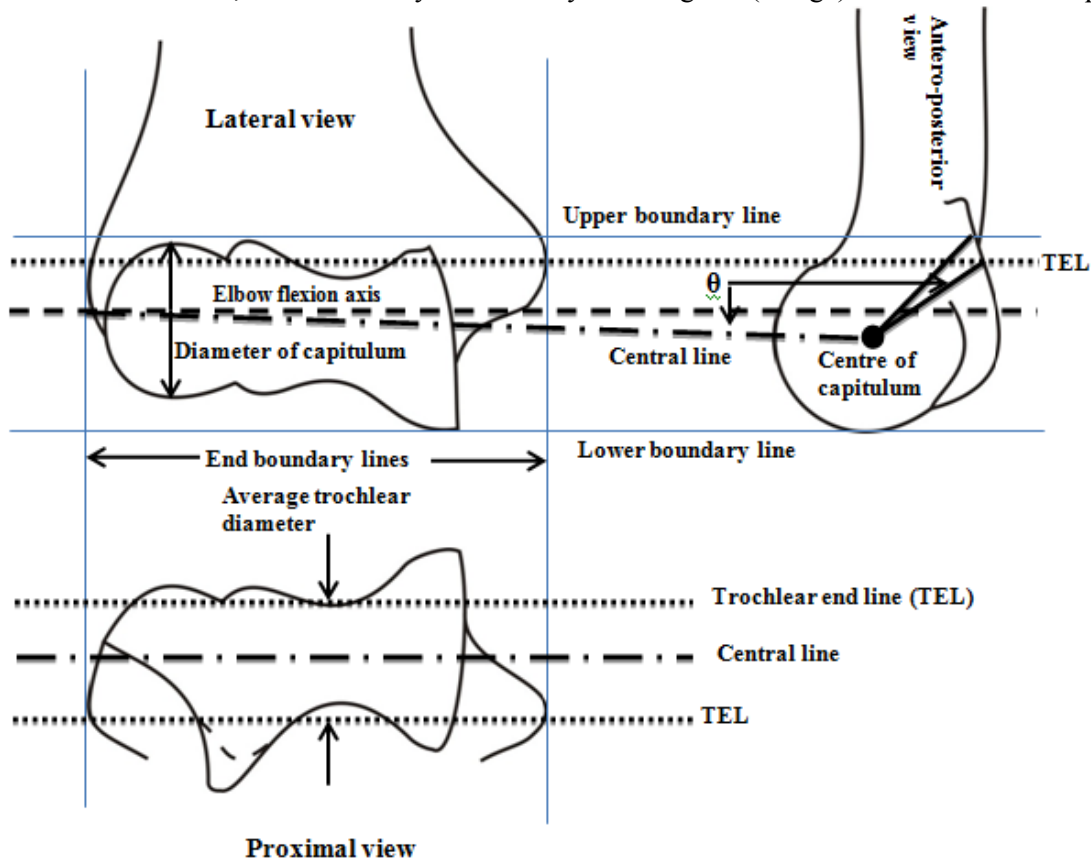


Figure 15C: Geometrical interpretation of distal end of humerus

(e) Geometrical Interpretation on Structure of Distal End of Humerus

Elbow flexion axis makes an angle θ with central line (Figures 15A & 15B) both medial and anterior view. The orientation relative to the humeral axis in the frontal plane and transepicondylar axis in the transverse plane of a right elbow is shown. Midpoint of condyles is indicated by \otimes (Figures 15A & 15B). The dotted line represents displaced (a) with respect to medial reference in the anterior view (Figure 15C) and (b) with respect to transepicondylar axis in the superior view (Figure 15B). Here angular displacement in each view is $\theta \approx 3^\circ$ (Figures 15A, 15B, 15C). The upper & lower TEL forms right circular cylinder with average diameter of trochlea.

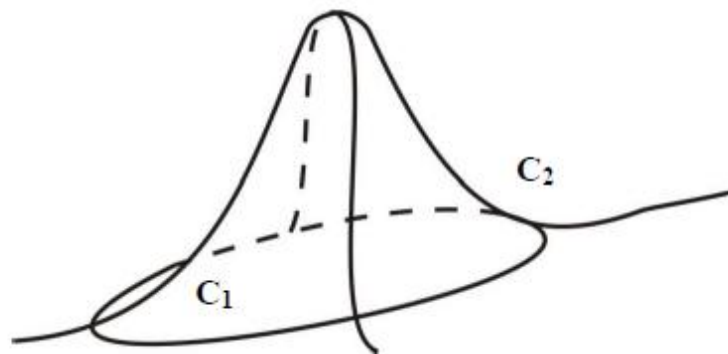


Figure 16: Geometrical view of notches over the trochlear end lines (both above and below)

Research Article

This figure (Figure 16) is showing notches over trochlear end lines as shown in the proximal view of the trochlea in Figure-15C. The curved surface C_1 is indicating the inner curve whereas C_2 is outer curve. Curvature of C_1 is less sharp than that of C_2 . The notches at both ends of the trochlea structurally restrict the movement of ulna i.e. within the spiral groove.

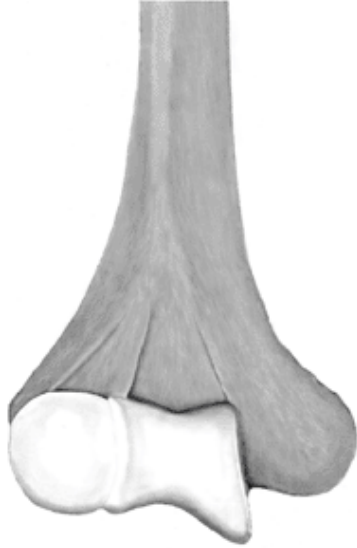


Figure 17A: Distal end of right humerus

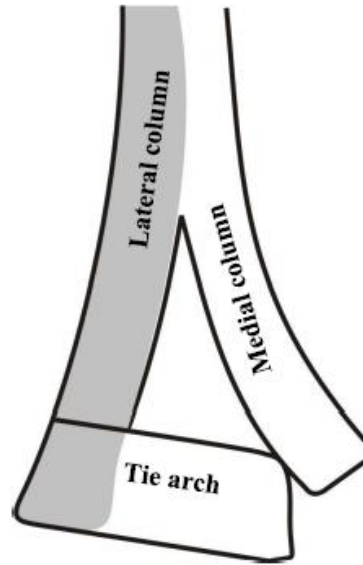


Figure 17B: Arrangement of right distal humerus on engineering view point

(f) Human Architectural Tie Arch

Capitulum is the distal part of the lateral column. The distal part of medial column is the non-articular medial epicondyle. The trochlea is positioned between the medial epicondyle and capitulum. This articular segment keep trochlea compressed and its functions architecturally is as a “tie arch” (Figure 17B).

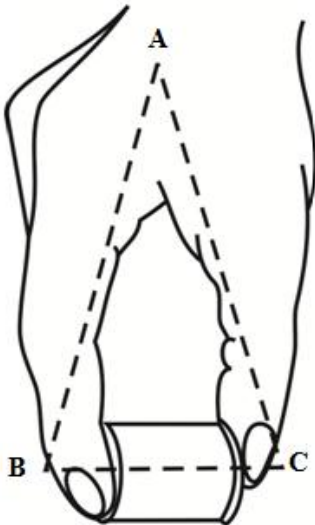


Figure 17C: Demonstration of distal end of humerus as holding trochlea & capitulum together by fingers



Figure 17D: Representing the lines of forces at the distal humerus

Research Article

The anatomy of the distal humerus is like as to a hand holding a threaded spool with strong support of the spool from each finger (Figure 17C). Likewise, the distal humerus has strong medial and lateral columns, which support the distal articular segment. The thin central area of the bone, made up of the olecranon and coronoid fossae, provide little bony support (Figure 17D). In both the figures we see equilibrium of triangular forces along \overline{AB} , \overline{BC} and \overline{CA} considering it to be in anticlockwise direction. This proves the stability of the structure even after forces exerted by the ulna due its movements on the spiral of trochlea.

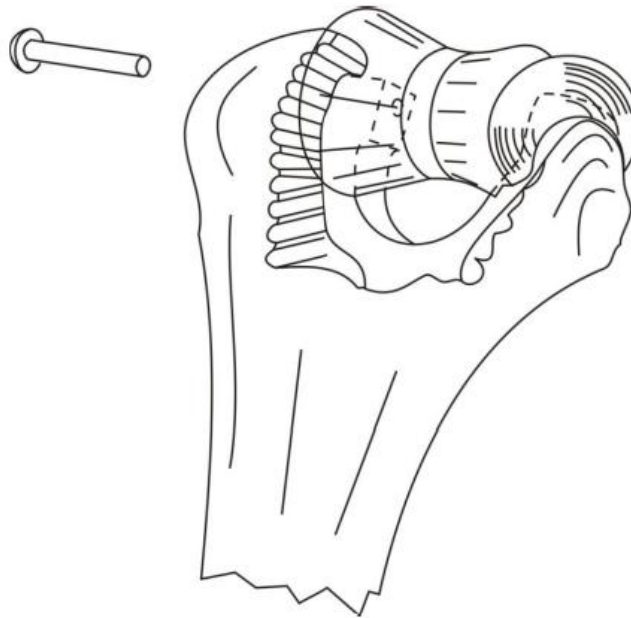


Figure 17E: Arrangement of Distal humerus on engineering point of view

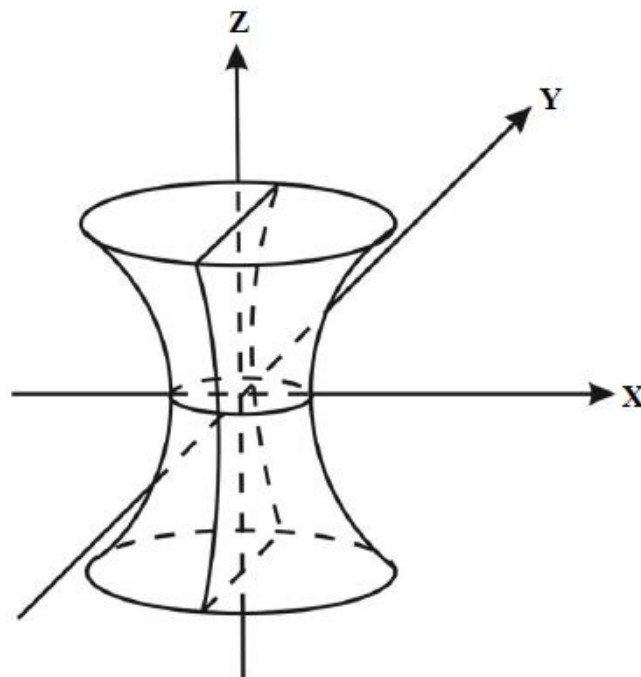


Figure 18: Hyperboloid on one sheet

Research Article

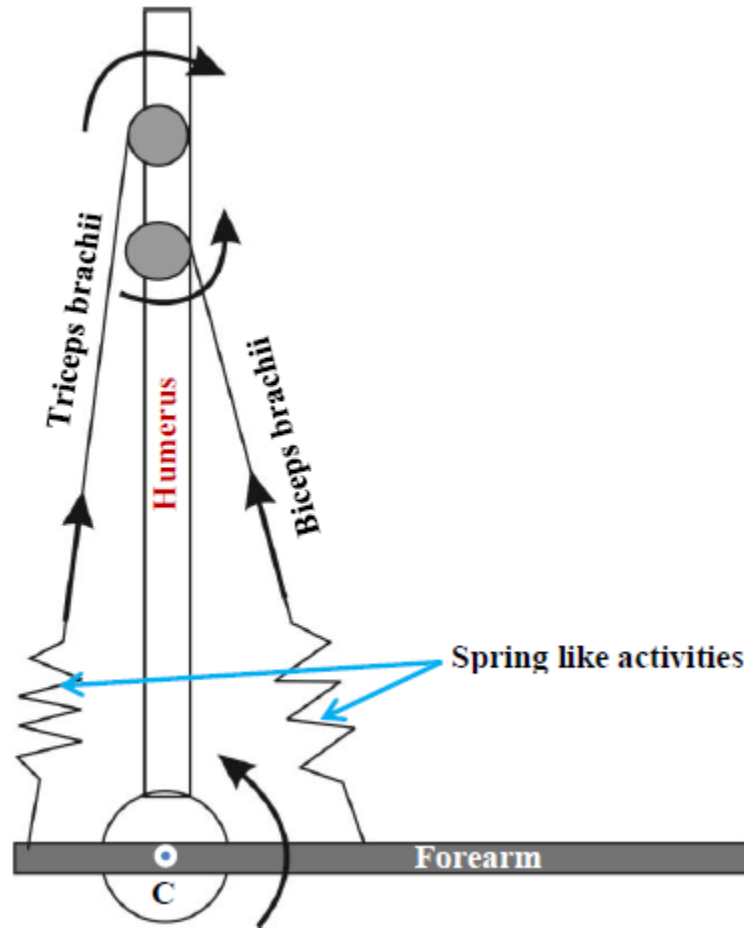


Figure 19A: Mechanical method of extension and flexion

(g) Mechanical and Geometrical Structure of Trochlea

According to mechanical demonstration (Figure 16E) we may consider trochlea, like *Damaru of Śiva* which is as hyperbolic cylinder i.e. hyperboloid of one sheet (Figure 18) whose equation is $\frac{x^2}{a^2} + \frac{y^2}{b^2} - \frac{z^2}{c^2} = 1$. Of course it is a right cylinder with circular base (Figure 15C). Its equation can be parameterised $x = a \cdot \cos u \cdot \cosh v$; $y = b \cdot \sin u \cdot \cosh v$; $z = c \cdot \sinh v$; where parameters u, v follows $0 \leq u < 2\pi$ and $-\infty \leq v \leq \infty$.

But transmission of forces through human structure follows the shortest and smoothest path which is Geodesics (An and Morrey, 1993). We know geodesics of any cylinder are helices i.e. spiral (Bell, 1965). So, path, through which ulnar ridge move, over the hyperboloid one sheet is accordingly spiral (Figure 3). Therefore mechanical structure can be mathematically deducted to be congruence with anatomical structure of trochlea.

(h) Mechanism on Activity of Muscles in Flexion-Extension

Extension of elbow depends on Triceps brachii whereas main flexor muscle is Biceps brachii. These two muscles organise rotational activities both in extension and in flexion. Muscles exert forces by extension- and contractions. So, force exertions have been demonstrated as spring like activities (Figure 19A). Resolution of extensor muscle force F_M has been demonstrated in Figure 13B.

Biceps brachii (PQ) operate radius in relation to humerus (Figure 19B). Let 'C' be the origin of the coordinate at the centre of the elbow joint. Here x -axis and z -axis are directed along the radius and the

Research Article

humerus respectively and y -axis is perpendicular to the xz -plane. B_F is a muscular force towards humerus. ' l ' is the muscle's moment-arm and ' M ' is the moment generated by the muscle. Actually M is the moment-vector and ' l ' is mechanical moment-arm. $\psi(\text{shi}) \propto B_F$. Q moves on circular path (Figure 19B).

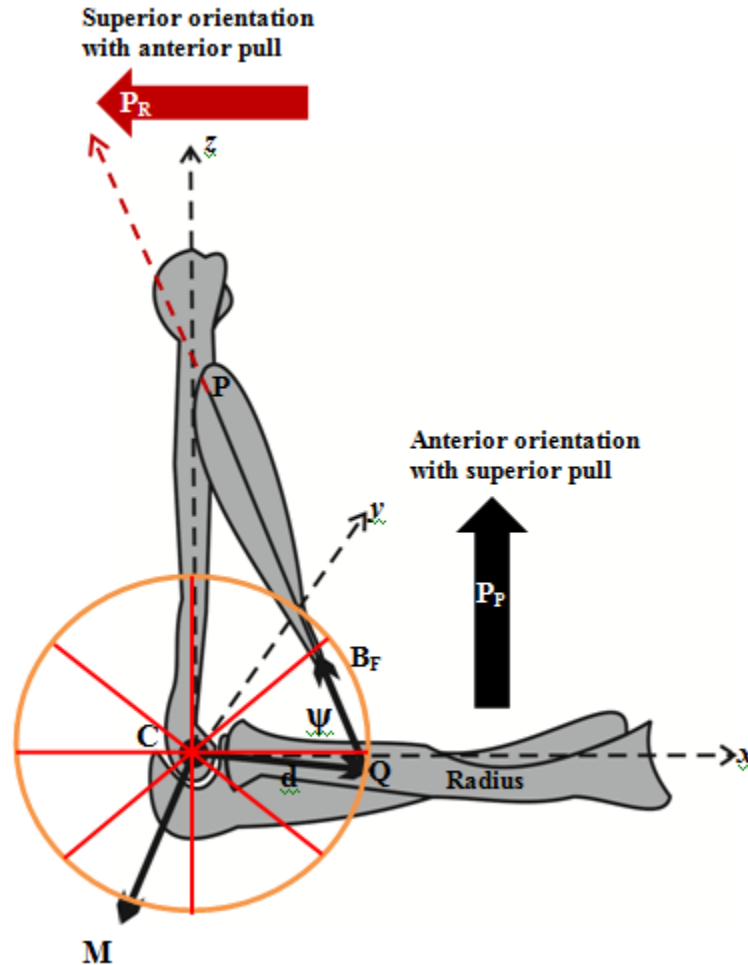


Figure 19B: Illustration of a three-dimensional elbow joint with a single muscle in sagittal plane

Biceps pull B_F can be resolved into P_R along the radius and P_P perpendicular direction to radius. A cyclic movement of pull has been shown in Figure 19B.

The muscles brachialis and brachioradialis operate ulna in relation to humerus. Figure 19C represents a simple two-dimensional geometric representation of the elbow joint at any angle with muscles activities where the paths of the brachialis and the brachioradialis also mentioned. Centre (C) of ulnar-joint is origin and insertion sites of muscles form triangles. In each muscle CM is perpendicular dropped from centre of rotation C on the muscles which determines the moments (Jinha *et al.*, 2006).

Figure 19C is representing both way rotation due to flexion-extension as well as supination-pronation but their axes of rotations are right-angle to each other.

Both the triangles (Figures 19E & 19F) are equiangular and this equiangularity shows the proportionality on the application force applications by the muscles.

Based on geometry, the value of moments produced by the activities of muscles can be calculated as: $D_{BRA} = CA =$ Distance of origin of Brachialis on the humerus (A) from the centre of rotation (C); $D_{BRD} = CD =$ Distance of insertion of Brachioradialis on the ulna (D) from the centre of rotation (C); $D_{HUS} = CE$

Research Article

= Distance of origin of Brachioradialis on the humerus (E) from the centre of rotation (C); $D_{ULA} = CB$ = Distance of insertion of Brachialis on the ulna (B) from the centre of rotation (C). Moment created by Brachialis at C = $M_{BRA} = AB \times CM = (AM + MB) \times CM = \{D_{BRA} \times \cos \beta + D_{ULA} \times \cos \alpha\} \times D_{ULA} \times \sin \alpha$ (or $D_{BRA} \times \sin \beta$); similarly, Moment created by Brachioradialis at C = $M_{BRD} = ED \times CM = (EM + MD) \times CM = \{D_{BRD} \times \cos \beta + D_{HUS} \times \cos \alpha\} \times D_{HUS} \times \sin \alpha$ (or $D_{BRD} \times \sin \beta$) (Dupuytren, 1835).

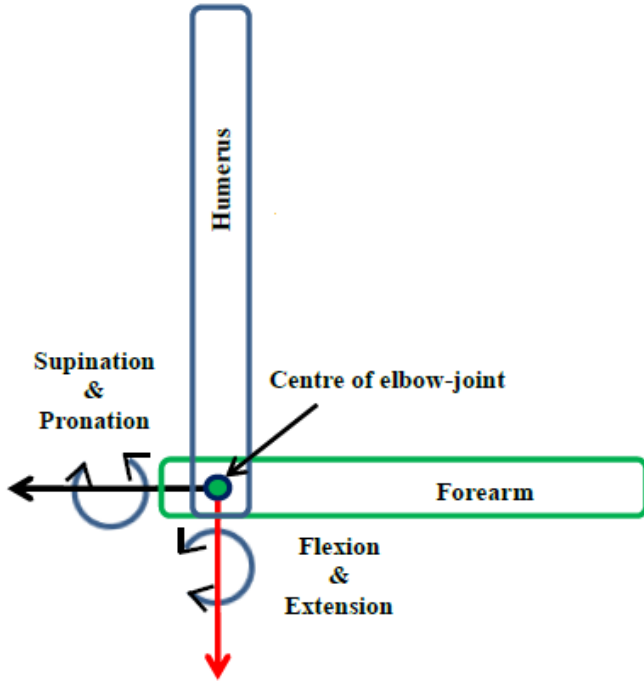


Figure 19C: Showing torques at centre of elbow-joint

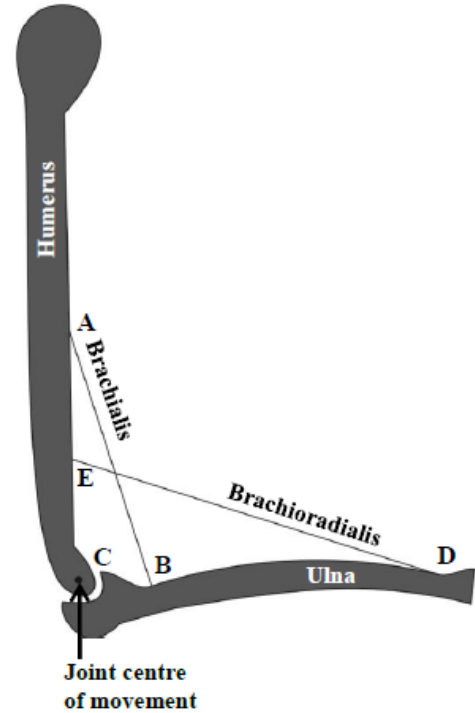


Figure 19D: Elbow-joint at an angle along with two muscles

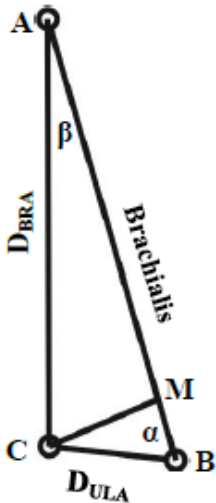


Figure 19E: Showing moment created by Brachialis

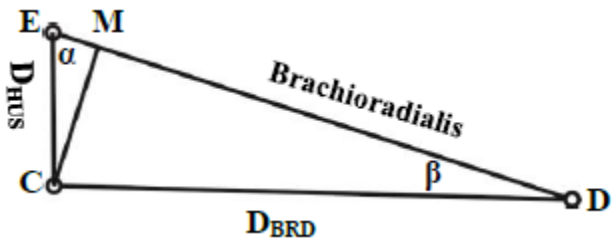


Figure 19F: Showing moment created by Brachioradialis

Now, in ΔABC : $(AC)^2 = (BC)^2 + (AB)^2 - 2 \cdot BC \cdot AB \cdot \cos \beta$

Research Article

$$\cos \beta = \frac{\{(BC)^2 + (AB)^2 - (AC)^2\}}{2 \cdot BC \cdot AB}$$

$$\sin \beta = \sqrt{1 - \cos^2 \beta}$$

$$CM = \frac{\{4 \cdot BC^2 \cdot AB^2 - (BC^2 + AB^2 - AC^2)^2\}^{\frac{1}{2}}}{2 \cdot AB}$$

Similarly, in ΔCDE : $CM = \frac{\{4 \cdot CE^2 \cdot DE^2 - (CE^2 + DE^2 - CD^2)^2\}^{\frac{1}{2}}}{2 \cdot DE}$

Moment = Force at muscle \times CM

(i) Application of Biomechanics

Mechanical load absorption between the plate and bone segment can only be assessed properly after adequate plate osteo synthesis. Strain reduction in the bony tissue depends on the cross-sectional area, geometrical form, and modulus of elasticity of the plate. The effect of plate positioning depends on bending stiffness.

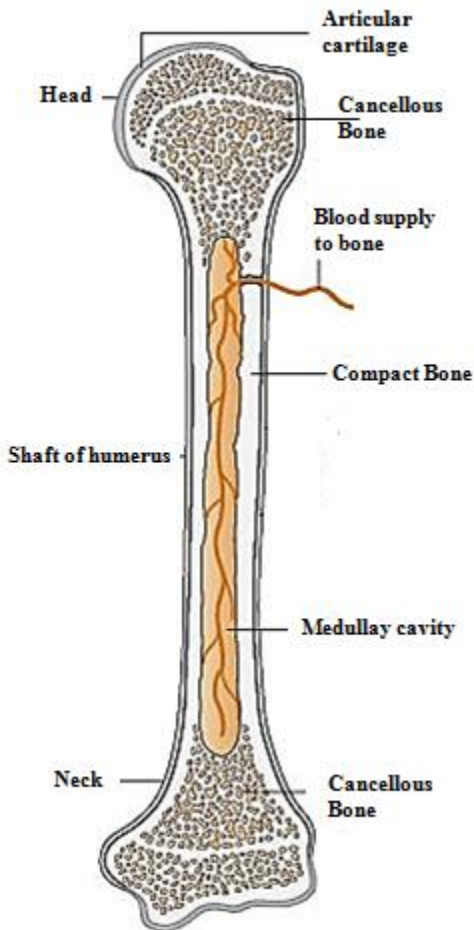


Figure 20: Showing structure bone at distal end of humerus

Figure 21: Use plates with twisted and bended as per structure at the distal end of humerus

The term plate is used when the length is considerably longer than the width and the thickness. The conditions of simple bending are as follows:

1. In bending the shear force will be zero i.e. no torsional or axial loads will be present.

Research Article

2. The material should be isotropic as well as homogeneous.
3. The material will obey Hook's Law.
4. The plate should be straight with constant cross section throughout the beam length.
5. The plate must have an axis of symmetry in the plane of bending.

Compressive and tensile forces develop along the plate axis which induces stresses. Compressive stress produced due to bending will be highest at the edges of the plate while the tensile stress will be lowest. These opposing maxima stresses are linearly dependent. A vertical line through the central point of bending is the neutral axis.

The bending stiffness (vide supra) is equal to the product of elastic modulus E and the area moment of inertia I of the plate. Thus bending stiffness $=E.I$.

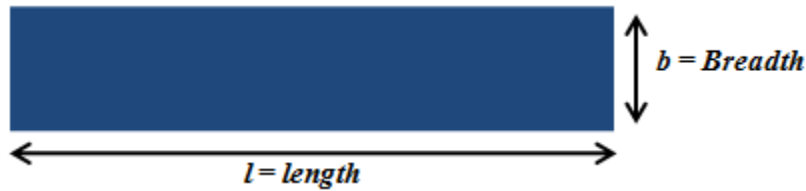


Figure 22: Plate

Elastic modulus $= \frac{\text{Stress}}{\text{Strain}}$; $I = \frac{l.b^3}{12}$; Stress = Force applied per unit area and Strain = Deformation per unit area (Figure 22). Thickness has been considered to be negligible in comparison with length and breadth for the plate.

According to elementary beam theory, the relationship between the applied bending moment M and the resulting curvature κ (kappa) of the beam is $M = E.I.\kappa = E.I.\frac{d^2\omega}{dx^2}$ where ω (omega) is the deflection of plate in x direction i.e. indirection of deformation.

Composite beams are common in applications like Automobile and orthopaedic applications etc. Unlike beams of Isotropic materials of composite plate may exhibit strong coupling between (1) Extensional; (2) Flexural and (c) Twisting mode of deformation.

The bending stiffness is maximum when bending moment acts in the direction of long axis of the plate. It is minimum when the plate bent breadthwise. It is assumed that the bone structure supporting the plate is capable of withstanding compressive load at that time.

The bending rigidity of the plate alone has only a minimal effect on the total stiffness affected by osteosynthesis.

Timoshenko's theory is effectively lowers the stiffness of beam to have larger deflection and his equation for bending of Isotropic beams of constant cross section:

$$E.I.\frac{d^4\omega(x)}{dx^4} = q(x) - \frac{E.I}{\zeta.A.S} \cdot \frac{d^2q(x)}{dx^2}$$

Where $q(x)$ = Applied load, $\omega(x)$ = deflection at the neutral axis x ; A = Area of cross-section; S = Shear modulus and ζ (zeta) = Shear correction factor. $= \frac{\text{Average shear strain on a section}}{\text{Shear strain at the centroid}}$ = This factor is used as because multi-layered plate and Shell finite elements have a constant shear distribution across thickness. This causes a decrease in accuracy especially for sandwich structures. This problem is overcome using shear correction factors. This is applicable to bending as well as twisting of plates.

(Centroid: In geometry and physics, the centroid or geometric centre of a two-dimensional region is, informally, the point at which a cardboard cut-out of the region could be perfectly balanced on the tip of a pencil (assuming uniform density and a uniform gravitational field). Formally, the centroid of a plane

Research Article

figure or two-dimensional shape is the arithmetic mean ("average") position of all the points in the shape. The definition extends to any object in n-dimensional space: its centroid is the mean position of all the points in all of the coordinate directions)

For tissues having large values of strain Lagrangian stress-strain equation is used as $\tau = a(e^{bv} - 1)$ where τ = stress = Force per unit area $= \frac{F}{A_0}$; v = strain $= \frac{\Delta L}{L}$ having F = Force applied, A_0 = Initial cross-sectional area, ΔL = change in length, L = Initial length and a, b are two parameters depending on the load exerted by muscle. The stress-strain relation may be converted into tangent-modulus relation by $\frac{d\tau}{dv} = b \cdot \tau + c$ where c is constant of integration and $c = ab$. It represents tangent modulus when $\tau \rightarrow 0$. Thus tangent modulus increases linearly with increasing stress (Bartel *et al.*, 2006).

(In solid mechanics, the tangent modulus is the slope of the compression stress-strain curve at any specified stress or strain. Below the proportional limit the tangent modulus is equivalent to Young's modulus. Above the proportional limit the tangent modulus varies with strain and is most accurately found from test data. The tangent modulus is useful in describing the behaviour of materials (muscles) that have been stressed beyond the elastic region).



Figure 23: Screw for spongy bone

(j) Regarding Selection of Screw

Full-threaded screws are usually used for better movement after fixation of fracture. Half threaded screw could only be used with partial success. For using screw we should consider the diameter of screw, the design of the thread. The material properties of both screw and the bone and length of the engagement of the screw are important. We can demonstrate for pull-out strength by a simple formula as:

$$P = L \cdot D \cdot \xi \cdot G$$

where P = Pull-out force; L = Length of the engagement of the screw; D = Outer diameter of the screw; ξ = Shearing strength of the bone; $G = \frac{\text{pitch of the screw}}{\text{depth of the thread}}$. Here G depends on the internal trabecular structure of the bone where screw will be inserted. This formula is based on the assumption that shear arising at fixation point will be absorbed by the threaded portion of the screw.

Research Article

CONCLUSION

In fracture, broken parts of the bone are put together. The broken parts are not simply fixed and compressed. We find that proper fixation with full threaded screw is competent to bear the load keeping the broken pieces together as it were. Half threaded screw would not do so in such case. The plates holding the screws would require adequate bending and twisting as per the details discussed in our article. *There is no class of injuries so frequently productive of discontent and perhaps so often the cause of litigation, as traumatic lesions of the elbow joint.* Henry Jacob Bigelow, Massachusetts General Hospital, Boston, 1868.

ACKNOWLEDGEMENT

I am thankful to Dr. Sailendra Bhattacharyya, FRCS & Dr. Sukhendu Sarkhel, MS of BORRC (Bhattacharyya Orthopaedics and Related Research Centre) Narayanpur, Kolkata - 700136 who requested me to deal with the context. This paper would not be possible without their encouragement

REFERENCES

- Adhikari Swapan Kumar (2011).** Trochanteric Fracture – Its Management Established by Mathematical Devices, *Indian Journal of Fundamental and Applied Life Sciences* **1**(3) 43-55.
- Albert H Burstein and Timothy M Wright (1994).** Fundamentals of Orthopaedic Biomechanics; Williams & Wilkins, Baltimore, USA.
- An K N and Morrey BF (1993).** Biomechanics of the elbow: 1st Edition. Philadelphia: WB Saunders.
- Andrew S Wong and Mark E Baratz (2009).** Elbow Fractures: Distal Humerus, *The Journal of Hand Surgery* **34**(1) 176-190.
- Bahl Ajay, Ranga Sharad and Sharma Rajnish (2001).** Basics of Biomechanics; Jaypee Brothers Medical Publishers (P) Ltd., New Delhi, India.
- Beasley A W (1982).** The Origins of Orthopaedics, *Journal of the Royal Society of Medicine* **75**(8) 648-655.
- Bigelow H J (1846).** Insensibility during Surgical Operations Produced by Inhalation, Boston.
- Chadwick E K J and Nicol A C (2000).** Elbow and Wrist Joint Contact Forces during Occupational Pick and Place Activities, *Journal of Biomechanics* **33**(5) 591-600.
- Das B C and Mukherjee B N (2001).** Differential Calculus **47**, U. N. Dhur & Sons Private Ltd., Kolkata - 700073, West Bengal, India.
- Donald L Bartel, Dwright T Davy and Tony M Keaveny (2006).** Orthopaedic Biomechanics, Pearson Education CE, New Delhi, India.
- Doornberg Job and Jupiter Jesse (2003).** Treatment of Elbow Fractures; Massachusetts General Hospital, *The Orthopaedic Journal at Harvard Medical School* **6** 95-99.
- Dupuytren G (1835).** Lectures on Clinical Surgery delivered in the Hotel Dieu of Paris, Washington, Green.
- Dupuytren G (1847).** On the Injuries and Diseases of Bone, 1st Edition, London, Sydenham Society.
- James Henry Breasted (1930).** The Edwin Smith Surgical Papyrus: Hieroglyphic Transliteration, Translation and Commentary **1 & 2**, the University of Chicago Press, Chicago, Illinois, USA.
- Jinha A, Ait-Haddou R, Binding P and Herzog W (2006).** Antagonistic of One-Joint in Three Dimensions Using Non-linear Optimisation, *Mathematical Biosciences* **202**(1) 57-70.
- Kapandji I A (1970).** The Physiology of Joints **1**, E. S. Livingstone, London.
- Knudson Duane (2007).** Fundamentals of Biomechanics, Springer, New York, USA.
- Lambotte A (1997).** The Beginning of Internal Fixation of Fractures (Osteosynthesis) in Belgium **2**, Bruxelles / Brussel, ASBL Acta Orthopaedica Belgica VZW.
- Levangie Pamela K and Norkin Cynthia C (2001).** Joint Structure and Function - A Comprehensive Analysis **3**, Jaypee Brothers, New Delhi, India.

Research Article

- Loney S L (1980).** An Elementary Treatise on the Dynamics of Particle and of Rigid Body, Metric Edition, Macmillan Company of India Limited, Calcutta, West Bengal, India.
- McWilliams B A, Sardelli M C and Tashijan R Z (2010).** A Functional Axis Based Upper Extremity Model and Associated Calibration Procedures, *Gait & Posture* **31**(2) 289-291.
- Milch H (1964).** Fractures and Fracture Dislocations of the Humeral Condyles, *Journal of Trauma* **15** 592-607.
- Robert J T Bell (1965).** An Elementary Treatise on Coordinate Geometry of Three Dimensions, Macmillan & Co. Ltd., London.
- Sadovaskii L E and Sadovaskii A L (1993).** Mathematics and Sports; American Mathematical Society, New York, USA.
- Santosh K Dutta and Debasis Datta (2008).** Applied Orthopaedic Biomechanics; BI Publications Pvt Ltd., New Delhi, India.
- Scudder C L and Cotton F J (1900).** The Treatment of Fractures, Philadelphia, W. B. Saunders.
- Shibendra Kuma Saha and Swapan Kumar Adhikari (2009).** Respiratory Aerodynamics - A Mathematical View of Prāṇāyāma, *Journal of the Asiatic Society* **LI**(3) 110-120.
- Shibendra Kumar Saha and Swapan Kumar Adhikari (2008).** Role of Fluid Mechanics in coronary artery blood-flow, *Journal of the Asiatic Society* **L**(1) 23-36.
- Swapan Kumar Adhikari (2000).** Human Femur & Mathematical Examination, *Indian Journal of Orthopaedics* **34**(4) 300-303.
- Swapan Kumar Adhikari (2001).** Pelvis – Distribution of Forces Through it by Mathematical Deductions, *Orthopaedic Update*, **11**(1) 5-10.
- Swapan Kumar Adhikari (2002).** Cervical Deformation – It's Causes and Its Deductions on Mathematical Basis, *Proceedings of the National Symposium* and University of Kalyani 1-25.
- Swapan Kumar Adhikari (2002).** The Role of Mathematics on Human Structure, Dipali Publication, Ghosuri, Howrah, West Bengal, India.
- Swapan Kumar Adhikari (2005).** Mechanical Role of Cruciate Ligaments in Flexion and Extension *Facta Universitatis* **17**(4) 367-372.
- Swapan Kumar Adhikari (2011).** Long Bones Are Not Just Props of the Structures Held by It, *Indian Journal of Fundamental and Applied Life Sciences* **1**(2) 98-106.
- Swapan Kumar Adhikari (2012).** Arthrokinematics Revisited at Knee, *International Journal of Basic and Applied Medical Sciences* **2**(2) 1-14.
- Swapan Kumar Adhikari, Shibendra Kumar Saha and Indra Datta (Mondal) (2011).** Sports Hints from the Skeleton and the Weight Bearing Joints, *Indian Journal of Fundamental and Applied Life Sciences* **1**(4) 73-83.
- Teresa R Duck, Cynthia E Dunning, April D Armstrong, James A Johnson, James A, Graham J W King and Graham J W (2003).** Application of Screw Displacement Axes to Qualify Elbow Instability, *Clinical Biomechanics* **18**(4) 303-310.
- Toh S, Tsubo K, Nishikawa S, Inoue S, Nakamura R and Narita S (2002).** Osteosynthesis for Non-union of the Lateral Humeral Condyle. *Clinical Orthopaedics* **405** 230-241.
- Tozeren and Aydin (2000).** Human Body Dynamics, Springer, New York, USA.
- Weatherburn C E (1964).** Differential Geometry of Three Dimensions, The English Language Book Society & Cambridge University Press.
- Wendy M Murray, Thomas S Buchanan and Scott L Delp (2002).** Scaling of Peak Moment Arms of Elbow Muscles with Upper Extremity Bone Dimensions, *Journal of Biomechanics* **35**(10) 19-26.